Carbon-Rich Metallacarboranes. 15.[1] Novel Metal-Promoted Cluster Fusion Reactions

Kent W. Piepgrass, Michael A. Curtis,† Xiaotai Wang, Xiangsheng Meng, Michal Sabat, and Russell N. Grimes*

Department of Chemistry, University of Virginia, Charlottesville, Virginia 22901

Received November 17, 1992

In contrast to our recently reported syntheses[2] of Co–M–Co tetradecker sandwich complexes (M = Co, Ni, Ru) via reactions of double-decker cobaltacarborane anions $Cp^*Co(Et_2C_2B_3H_3X)^-$ (**1**$^-$, X = H, Me, Cl, Br, acetyl) with metal halides, reactions of the anions having X = H, Me, Et, or Cl with $FeCl_2$ did not produce the intended Co–Fe–Co tetradeckers. Instead, oxidative fusion of the CoC_2B_3 units occurred, generating tetracarbon metallacarboranes $Cp^*_2Co_2Et_4C_4B_6H_4X_2$ (**3a–d**), which have been characterized via NMR, IR, and mass spectroscopy, supported by X-ray crystallographic analyses of the parent (**3a**) and dichloro (**3d**) clusters. These compounds have an open $Co_2C_4B_6$ 12-vertex cage structure that is a fragment of a 16-vertex T_d closo polyhedron, a geometry that was previously unknown in cluster chemistry and (in these species) is not consistent with the widely applied skeletal-electron counting rules. Moreover, it differs from the $Co_2C_4B_6$ cage structures of several known cobaltacarboranes.[4] An attempt to prepare a diiodo Co–Ni–Co tetradecker complex from **1**$^-$ (X = I) with $NiBr_2$ gave instead the dimer $[Cp^*Co(Et_2C_2B_3H_3)]_2$ (**6**), which was shown by X-ray crystallography to have an edge-fused structure in which the two C_2B_3 rings are mutually tilted. A centrosymmetric isomer of this dimer (**8**) having coplanar C_2B_3 rings with the Cp^*Co units on opposite sides of the ring plane was isolated from a reaction of **1**$^-$ (X = H) with $CoCl_2$ and Cp_2Co and characterized by X-ray diffraction. Also isolated from this reaction were a dimer of a different type (joined via a single B–B bond), $[Cp^*Co(Et_2C_2B_3H_4)]_2$ (**9**), together with previously reported[2a] Co–Co triple-decker and Co–Co–Co tetradecker products. The implications of the formation and structures of the fused and partially fused products found in this work are discussed in terms of multidecker stacking mechanisms and skeletal electron-counting theory.

Introduction

In recent publications[2] we have described the synthesis and characterization of tetradecker sandwich complexes (**2**) via coordination of two *nido*-$Cp^*CoC_2B_3$ metallacarborane units ($Cp^* = \eta^5$-C_5Me_5) to a central metal (M), as shown in Scheme I. These stacking reactions are highly sensitive to the nature of the substituent X on the middle boron atom (B5) of the metallacarborane substrate; strongly electron-withdrawing X groups (Cl, Br, acetyl) produce good yields of the corresponding tetradeckers following separation on silica columns in air. Tetradecker sandwiches in which X = CH_3 or H have also been isolated, in the latter case only when contact with silica was avoided. In contrast, the B5–ethyl complex generates no tetradeckers (or any detectable products) on treatment with metal reagents.[2a]

Clearly, the stacking process is mechanistically nontrivial and is sensitive to the choice of substituent groups, metals, and workup conditions.[2a] The formation of tetradeckers competes with other possible reactions, of which the two most important are (1) reprotonation of the cobaltacarborane anion to form neutral $Cp^*Co(Et_2C_2B_3H_4X)$ complexes and (2) fusion of two CoC_2B_3 units to generate $Co_2C_4B_6$ clusters. In this paper we describe reactions of the latter reaction type that produced several structurally novel cage products.

Results and Discussion

Formation of $Co_2C_4B_6$ Clusters. Metal-promoted oxidative fusion of boron-containing clusters has been known since 1974[3a]

Scheme I

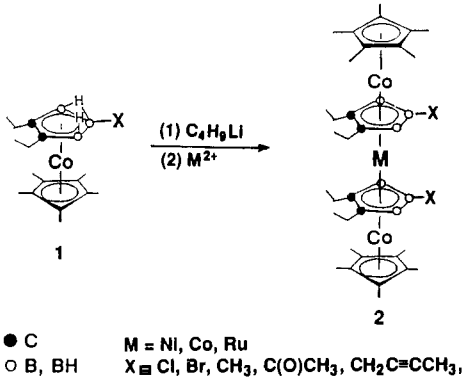

and has been extensively studied in our group.[3b–e] It has been observed with boron hydrides, carboranes, metallacarboranes, and metallaboranes and usually involves a net conversion of two dinegative substrate anions to a neutral fusion product, e.g.,

$$2\ nido\text{-}R_2C_2B_4H_4^{2-} \xrightarrow[-4e]{M^{n+}} R_4C_4B_8H_8$$

An equivalent process is the oxidation of two mononegative anions to a neutral product and hydrogen gas, e.g.,

$$2\ nido\text{-}R_2C_2B_4H_5^- \xrightarrow[-2e]{M^{n+}} R_4C_4B_8H_8 + H_2$$

The corresponding *nido*-metallacarborane anions such as

† Summer 1991 undergraduate research student from Indiana University Southeast, New Albany, IN 47150.

(1) Part 14: Wang, Z.-T.; Sinn, E.; Grimes, R. N. *Inorg. Chem.* **1985**, *24*, 834.

(2) (a) Piepgrass, K. W.; Meng, X.; Hölscher, M.; Sabat, M.; Grimes, R. N. *Inorg. Chem.* **1992**, *31*, 5202. (b) Piepgrass, K. W.; Davis, J. H., Jr.; Sabat, M.; Grimes, R. N. *J. Am. Chem. Soc.* **1991**, *113*, 681.

(3) (a) Maxwell, W. M.; Miller, V. R.; Grimes, R. N. *J. Am. Chem. Soc.* **1974**, *96*, 7116. (b) Grimes, R. N. *Chem. Rev.* **1992**, *92*, 251. (c) Grimes, R. N. Synthetic Strategies in Boron Cage Chemistry. In *Advances in Boron and the Boranes* [*Mol. Struct. Energ. Vol. 5*]; Liebman, J. F.; Greenberg, A.; Williams, R. E., Eds.; VCH Publishers, Inc.: New York, 1988; Chapter 11, pp 235–263. (d) Grimes, R. N. *Adv. Inorg. Chem. Radiochem.* **1983**, *26*, 55 and references therein. (e) Maynard, R. B.; Grimes, R. N. *J. Am. Chem. Soc.* **1982**, *104*, 5983.

0020-1669/93/1332-2156$04.00/0

Scheme II

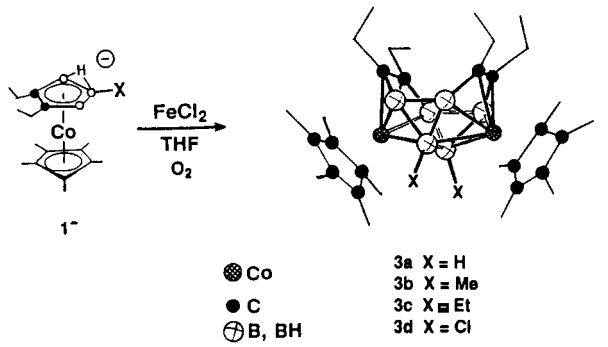

$Cp^*Co(Et_2C_2B_3H_4)^-$ ($\mathbf{1}^-$) similarly have been shown to undergo fusion:[4]

$$2LCo(R_2C_2B_3H_4)^- \xrightarrow[-2e]{M^{n+}} L_2Co_2R_4C_4B_6H_6 \text{ (several isomers)} + H_2$$

$$L = Cp, Cp^*; R = H, \text{alkyl}$$

In the present work, fusion was observed in a number of attempted tetradecker syntheses, for example, when Fe^{2+} was employed as the complexing reagent. Remarkably, all efforts to prepare tetradecker sandwich complexes incorporating Fe between two metallacarborane units have failed,[2a] often generating fusion products instead. An illustrative example is the reaction shown in Scheme II. The tetracarbon metallacarborane clusters $Cp^*_2Co_2Et_4C_4B_6H_4X_2$ (**3a–d**) were obtained in low to moderate yields (8–44%) as dark brown air-stable solids, following bridge-deprotonation of the substituted cobaltacarboranes **1a–d**, reaction with $FeCl_2$ in THF, and workup in air on silica columns. In each case, other products were detected but could not be satisfactorily characterized; however, mass spectra of the product mixtures gave no indication of the expected iron-centered tetradecker species **2**. The fact that fused rather than tetradecker products are observed when Fe^{2+} is employed, in contrast to the reactions involving Co^{2+} and Ni^{2+}, has been discussed earlier.[2a] A possible rationale is that iron-centered tetradeckers are in fact formed initially but that the B–B edges of opposing C_2B_3 rings are drawn together by the relatively electron-poor iron atom; this may induce interligand B–B bonding and thereby initiate fusion of the $Cp^*CoC_2B_3$ units. The observation of a Co–Ru–Co tetradecker that is significantly bent in the middle[2a] lends some support to this idea.

Compounds **3a** and **3d** were characterized via ^1H and ^{11}B NMR, infrared, UV–visible, and mass spectra (Table I and Experimental Section), while the identities of **3b** and **3c** were postulated from mass spectra, assuming analogous cage structures. These species are $Co_2C_4B_6$ cage isomers of the known clusters $Cp_2Co_2R_4C_4B_6H_6$ (R = H, Me), three of which were isolated and two (discussed below) characterized by X-ray diffraction.[4] The NMR data on the new complexes, however, indicated cage structures different from those of the earlier species. Accordingly, X-ray structure determinations were conducted on the parent cluster **3a** and its dichloro derivative **3d**. Relevant data on the structure determinations and refinements are collected in Table II, bond distances and angles are given in Tables III and IV, and the molecular geometries are shown in Figure 1. To all intents and purposes the two molecules exhibit identical cage structures, as can be seen by comparing corresponding bond distances and angles. Particularly noteworthy in both molecules are the unusually short

Table I. ^{11}B and ^1H FT NMR Data

115.8-MHz ^{11}B NMR Data

compd	$\delta^{a,b}$	rel areas
$(C_5Me_5)_2Co_2Et_4C_4B_6H_6$ (**3a**)	49.9, 29.8	1:2
$(C_5Me_5)_2Co_2Et_4C_4B_6H_4Cl_2$ (**3d**)	43.6, 28.2	1:2
$[(C_5Me_5)Co(Et_2C_2B_3H_3)]_2$, bent isomer (**6**)	50.9, −3.5	1:2
$[(C_5Me_5)Co(Et_2C_2B_3H_3)]_2$, "planar" isomer (**8**)	33.1, 7.1 (78), −4.4 (80)	1:1:1
$[(C_5Me_5)Co(Et_2C_2B_3H_4)]_2$ (**9**)	6.1, 3.8	1:2
$(C_5Me_5)Co(Et_2C_2B_3H_3)Co(C_5H_5)$ (**10**)	52.9 (145), 7.8 (150)	1:2

300-MHz ^1H NMR Data

compd	δ^{c-f}
3a	2.06 m (ethyl CH_2), 1.71 m (ethyl CH_2), 1.59 s (C_5Me_5), 0.99 t (ethyl CH_3)
3d	1.73 m (ethyl CH_2), 1.45 s (C_5Me_5), 1.04 t (ethyl CH_3)
6	[2.24 m, 2.09 m, 2.01 m, 1.73 m] (ethyl CH_2), 1.85 s (C_5Me_5), 1.10 t (ethyl CH_3), 0.99 t (ethyl CH_3), −2.8 sb (B–H–B)
8	2.27 m (ethyl CH_2), 2.08 m (ethyl CH_2), 1.58 s (C_5Me_5), 1.28 t (ethyl CH_3), 1.24 t (ethyl CH_3), −8.4 sb (B–H–B)
9	2.14 m (ethyl CH_2), 2.01 m (ethyl CH_2), 1.65 s (C_5Me_5), 1.17 t (ethyl CH_3), 1.14 t (ethyl CH_3), [−5.5 sb, −5.6 sb, −6.0 sb] (B–H–B)
10	4.35 s (C_5H_5), 2.69 m (ethyl CH_2), 1.59 m (ethyl CH_3), 1.57 s (C_5Me_5)

[a] Shifts relative to $BF_3{\cdot}OEt_2$, positive values downfield. H–B coupling is given in parentheses when resolved. [b] Dichloromethane solution. [c] $CDCl_3$ solution. Integrated peak areas in all cases are consistent with the assignments given. Legend: m = multiplet, s = singlet, sb = broad singlet, d = doublet, t = triplet, q = quartet. [e] $B–H_{terminal}$ resonances are broad quartets and mostly obscured by other signals. [f] Shifts relative to $(CH_3)_4Si$.

cage C–C bonds (ca. 1.42 Å) and long B–B edges on the open faces (B6–B9* in **3a**; B5–B6 and B9–B10 in **3d**), whose values range from 1.87 to 1.90 Å. In each species, both of the six-membered C_2B_4 rings bound to cobalt are planar within experimental error, and the dihedral angles formed by these planes are closely similar (72.4° in **3a** and 69.7° ion **3d**). Thus, the **3a**/**3d** cage structure can be described as a pair of hexagonal pyramidal CoC_2B_4 units sharing a common B–B edge. This geometry is clearly different from those of the previously characterized[4] $Co_2C_4B_6$ cage isomers **4** and **5**, depicted in Figure 2, and to our knowledge is unprecedented in cluster chemistry. However, it is curious to note that the **3a**/**3d** structure was proposed[4a] by Pipal and Grimes in 1979 as a reaction intermediate in the formation of **4** and **5**; it has never been seen experimentally until the current study.

The cluster geometry of **3a** and **3d** raises intriguing questions. For one thing, it clearly violates the well-established skeletal electron-counting theory[5] ("Wade's rules"), which predicts a nido structure (a 13-vertex polyhedron minus one vertex) for these clusters. This follows from the two Cp*Co, six BH (or B–Cl), and four C–ethyl units which furnish 2, 2, and 3 electrons each, for a total of 28; since the number of vertices (n) is 12, the cage is in the $2n + 4$ electron class and hence should be nido. In fact, the **3a**/**3d** geometry is a fragment of a 16-vertex closo polyhedron of tetrahedral symmetry (point group T_d), as is clearly seen in Figure 3. Thus, the two metal atoms in the $Co_2C_4B_6$ cage occupy 6-coordinate vertices, which correspond to two of the four such vertices that are present in the parent closo polyhedron. The

(4) (a) Wong, K.-S.; Bowser, J. R.; Pipal, J. R.; Grimes, R. N. *J. Am. Chem. Soc.* **1978**, *100*, 5045. (b) Pipal, J. R.; Grimes, R. N. *Inorg. Chem.* **1979**, *18*, 1936.

(5) (a) Wade, K. *Adv. Inorg. Chem. Radiochem.* **1976**, *18*, 1. (b) Mingos, D. M. P. *Acc. Chem. Res.* **1984**, *17*, 311. (c) Mingos, D. M. P.; Wales, D. J. *Introduction to Cluster Chemistry*; Prentice Hall: Englewood Cliffs, NJ, 1990.

Table II. Experimental X-ray Diffraction Parameters and Crystal Data

compd	**3a**	**3d**	**6**	**8**
empirical formula	$Co_2C_{32}B_6H_{56}$	$Co_2Cl_2C_{32}B_6H_{54}$	$Co_2C_{32}B_6H_{56}$	$Co_2C_{32}B_6H_{56}$
fw	623.5	692.4	623.5	623.5
cryst color, habit	red plate	black prism	red needle	yellow plate
cryst dimens, mm	0.47 × 0.36 × 0.22	0.47 × 0.32 × 0.30	0.42 × 0.25 × 0.22	0.38 × 0.32 × 0.15
space group	$C2/c$	$Pca2_1$	$C2/c$	$P2_1/n$
a, Å	20.010(2)	15.011(4)	10.679(2)	12.967(2)
b, Å	10.708(2)	18.209(5)	13.433(3)	8.966(3)
c, Å	15.524(3)	12.528(3)	24.511(5)	14.329(2)
β, deg	107.79(2)	90.00	100.71(2)	100.92(1)
V, Å^3	3167	3424	3455	1636
Z	4	4	4	2
μ, cm^{-1} (Mo Kα)	10.66	11.46	9.77	10.32
transm factors	0.85–1.00	0.87–1.00	0.61–1.36	0.85–1.00
D(calcd), g cm^{-3}	1.309	1.343	1.199	1.266
$2\theta_{max}$	50	50	50	50
no. of reflcns measd	3056	2773	2686	3243
no. of reflcns obsd[a]	2157	2357	1935	2141
R	0.031	0.033	0.048	0.029
R_w	0.042	0.045	0.075	0.039
largest peak in final diff map, e/Å^3	0.35	0.33	0.34	0.38

[a] $I > 3\sigma(I)$.

Table III. Bond Distances and Selected Bond Angles for $Cp^*_2Co_2Et_4C_4B_6H_6$ (**3a**)

Bond Distances, Å			
Co–C7	2.161(3)	C8M–C8E	1.520(4)
Co–C8	2.152(3)	C8–B9	1.527(5)
Co–C1R1	2.083(3)	C1R1–C1R2	1.432(4)
Co–C1R2	2.103(3)	C1R1–C1R5	1.413(4)
Co–C1R3	2.112(3)	C1R1–C1R6	1.503(4)
Co–C1R4	2.101(3)	C1R2–C1R3	1.414(4)
Co–C1R5	2.101(3)	C1R2–C1R7	1.498(4)
Co–B3	2.172(3)	C1R3–C1R4	1.425(4)
Co–B3*	2.185(3)	C1R3–C1R8	1.496(4)
Co–B6	2.128(3)	C1R4–C1R5	1.418(4)
Co–B9	2.132(3)	C1R4–C1R9	1.494(4)
C7M–C7	1.522(4)	C1R5–C1R10	1.482(4)
C7M–C7E	1.520(4)	B3–B3*	1.772(7)
C7–C8	1.431(4)	B3–B6	1.765(5)
C7–B6	1.526(4)	B3–B9*	1.766(5)
C8M–C8	1.522(4)	B6–B9*	1.886(5)
Selected Bond Angles, deg			
C7–C7M–C7E	109.7(2)	C8M–C8–B9	115.8(3)
Co–C7–C7M	132.7(2)	C7–B6–B9*	121.9(2)
C7M–C7–C8	120.6(3)	C8–B9–B6*	118.5(2)
C7M–C7–B6	114.4(3)	C1R2–C1R1–C1R5	108.6(3)
C8–C7–B6	124.5(3)	C1R1–C1R2–C1R3	107.6(3)
C8–C8M–C8E	111.0(2)	C1R2–C1R3–C1R4	107.8(3)
Co–C8–C8M	130.1(2)	C1R3–C1R4–C1R5	108.6(3)
C7–C8–C8M	120.1(3)	C1R1–C1R5–C1R4	107.4(3)
C7–C8–B9	123.6(3)		

parent 16-vertex cluster geometry is itself rare in chemistry, having been found experimentally only recently[6] as a discrete In_{16} cluster in a solid-state compound, $Na_7In_{11.8}$. As far as we know, neither the closo polyhedron nor a major fragment of it has heretofore been found in a boron cluster, although the T_d closo geometry has been proposed for the unknown borane $B_{16}H_{16}$, which was calculated to be stable as a neutral entity.[7]

Since the **3a**/**3d** structure is formally derived by removal of four contiguous vertices from the 16-vertex T_d cage, it would fall into the klado class of polyhedra, which under Wade's rules would require $2n + 10$ skeletal electrons, or 6 more than are actually present. How can one account for this major deviation from polyhedral bonding theory? We will attempt no detailed analysis here but wish to make two points. First, of the four established $Co_2C_4B_6$ cage structures (Figures 1 and 2), one of them (**5**) *is* in fact a nido 12-vertex species as expected from Wade's rules. Our judgment is that **5** may well represent the thermodynamically preferred geometry but that the other isomers are locked into kinetically determined arrangements which reflect their mode of synthesis. This is a situation that has been observed in previous studies in our laboratory and, we believe, in other groups as well. For example, work in this laboratory demonstrated[8] that a 14-vertex, 30-electron $Fe_2C_4B_8$ cage system, which according to Wade's rules should exhibit a closo polyhedral geometry, achieves this structure *only on prolonged heating at elevated temperature* (*300* °C); under less energetic conditions, other isomers having highly irregular non-Wade open-cage geometries are observed.

This leads to our second point, which is that polyhedral skeletal bonding theory, in its current stage of development, is not applicable to kinetically stabilized cage structures. That is, Wade's rules provide a reasonable guide to the thermodynamically *favored* structure but cannot, in general, deal with intermediate species whose shapes reflect primarily the reaction pathways and the structures of the precursor compounds. In the case of complexes **3a** and **3d**, this is particularly evident: the conjoining of two CoC_2B_3 fragments at their respective B–B edges, with each C_2B_3 ring expanded to a C_2B_4 planar ring by insertion of a boron from the other unit, leads directly to the cage structure found in **3a–d**. The fact that this framework fails to undergo facile rearrangement to, say, the predicted nido geometry of complex **5** suggests kinetic stabilization associated with the high C_{2v} symmetry of the **3** cage.

Formation of "Edge-Fused" Dimers. As generally understood, the term "fusion" implies the formation of a single open or closed cluster framework from two precursor units, while the joining of two units by one bond (e.g., B–B) is described as "coupling". Intermediate situations are known, in which two cages are linked via more than one electron-pair bond but retain their separate structural identity, as in the borane dimers $B_{18}H_{22}$[9] and $B_{12}H_{16}$.[10] The present study led to the isolation of two such species which were crystallographically characterized.

An attempted synthesis of a diiodo Co–Ni–Co tetradecker sandwich from the B5-iodo double-decker complex **1e** (Scheme III), which was expected to proceed analogously to the preparation of the corresponding dichloro and dibromo species[2a] as in Scheme I, instead gave the dimer $[Cp^*Co(Et_2C_2B_3H_3)]_2$ (**6**) as the only isolable product other than a trace of an iodo triple-decker, $Cp^*Co(Et_2C_2B_3H_2I)CoCp^*$ (not shown). No evidence of a Co–

(6) Sevov, S. C.; Corbett, J. D. *Inorg. Chem.* **1992**, *31*, 1895.
(7) Bicerano, J.; Marynick, D. S.; Lipscomb, W. N. *Inorg. Chem.* **1978**, *17*, 3443.
(8) (a) Maxwell, W. M.; Weiss, R.; Sinn, E.; Grimes, R. N. *J. Am. Chem. Soc.* **1977**, *99*, 4016. (b) Pipal, J. R.; Grimes, R. N. *Inorg. Chem.* **1978**, *17*, 6.
(9) Simpson, P. G.; Folting, K.; Dobrott, R. D.; Lipscomb, W. N. *J. Chem. 4Phys.* **1963**, *39*, 2339.
(10) Brewer, C. T.; Swisher, R. G.; Sinn, E.; Grimes, R. N. *J. Am. Chem. Soc.* **1985**, *107*, 3558.

Table IV. Bond Distances and Selected Bond Angles for $Cp^*_2Co_2Et_4C_4B_6H_4Cl_2$ (**3d**)

	Bond Distances, Å		
Co1–C7	2.166(5)	C1R1–C1R2	1.434(7)
Co1–C8	2.159(5)	C1R1–C1R5	1.421(6)
Co1–C1R1	2.115(4)	C1R1–C1R6	1.485(7)
Co1–C1R2	2.135(5)	C11–C12	1.420(7)
Co1–C1R3	2.119(5)	C11–B10	1.553(8)
Co1–C1R4	2.096(4)	C1R2–C1R3	1.397(7)
Co1–C1R5	2.103(5)	C1R2–C1R7	1.511(7)
Co1–B3	2.257(4)	C12M–C12	1.530(7)
Co1–B4	2.263(5)	C12M–C12E	1.48(1)
Co1–B6	2.129(5)	C12–B5	1.508(7)
Co1–B9	2.133(5)	C1R3–C1R4	1.438(7)
Co2–C11	2.162(5)	C1R3–C1R8	1.493(8)
Co2–C12	2.151(5)	C1R4–C1R5	1.413(7)
Co2–C2R1	2.134(5)	C1R4–C1R9	1.486(7)
Co2–C2R2	2.161(5)	C1R5–C1R10	1.508(6)
Co2–C2R3	2.152(5)	C2R1–C2R2	1.408(8)
Co2–C2R4	2.151(5)	C2R1–C2R5	1.431(7)
Co2–C2R5	2.141(5)	C2R1–C2R6	1.475(8)
Co2–B3	2.231(5)	C2R2–C2R3	1.468(8)
Co2–B4	2.211(5)	C2R2–C2R7	1.463(9)
Co2–B5	2.099(5)	C2R3–C2R4	1.403(8)
Co2–B10	2.109(5)	C2R3–C2R8	1.484(9)
Cl3–B3	1.848(5)	C2R4–C2R5	1.406(8)
Cl4–B4	1.848(5)	C2R4–C2R9	1.510(8)
C7M–C7	1.526(7)	C2R5–C2R10	1.491(8)
C7M–C7E	1.42(1)	B3–B4	1.751(6)
C7–C8	1.409(7)	B3–B5	1.754(7)
C7–B6	1.526(7)	B3–B6	1.759(7)
C8M–C8	1.526(7)	B4–B9	1.765(7)
C8M–C8E	1.40(1)	B4–B10	1.746(7)
C8–B9	1.528(8)	B5–B6	1.904(8)
C11M–C11	1.510(8)	B9–B10	1.867(7)
C11M–C11E	1.43(1)		
	Selected Bond Angles, deg		
C7–C7M–C7E	116.1(7)	C8–B9–B10	118.8(4)
Co1–C7–C7M	130.1(4)	C11–B10–B9	116.8(4)
C7M–C7–C8	120.4(5)	Cl3–B3–B4	127.1(3)
C7M–C7–B6	115.7(5)	Cl3–B3–B5	111.8(3)
C8–C7–B6	123.3(4)	Cl3–B3–B6	111.4(3)
C8–C8M–C8E	115.3(7)	Co1–B3–Cl3	111.3(2)
Co1–C8–C8M	132.4(4)	Co2–B3–Cl3	112.1(2)
C7–C8–C8M	119.3(5)	Co2–B4–Cl4	112.0(2)
C7–C8–B9	124.0(4)	Co1–B4–Cl4	110.9(2)
C8M–C8–B9	116.4(5)	Cl4–B4–B3	126.9(3)
C11–C11M–C11E	114.6(7)	Cl4–B4–B9	111.8(3)
Co2–C11–C11M	131.4(4)	Cl4–B4–B10	111.5(3)
C11M–C11–C12	120.0(5)	C1R2–C1R1–C1R5	107.3(4)
C11M–C11–B10	116.8(5)	C1R1–C1R2–C1R3	108.0(4)
C12–C11–B10	122.6(4)	C1R2–C1R3–C1R4	108.9(4)
C12–C12M–C12E	111.2(6)	C1R3–C1R4–C1R5	106.8(4)
Co2–C12–C12M	132.4(4)	C1R1–C1R5–C1R4	108.9(4)
C11–C12–C12M	119.8(5)	C2R2–C2R1–C2R5	108.2(5)
C11–C12–B5	124.1(4)	C2R1–C2R2–C2R3	107.3(5)
C12M–C12–B5	115.8(5)	C2R2–C2R3–C2R4	106.9(5)
C12–B5–B6	117.5(4)	C2R3–C2R4–C2R5	109.4(5)
C7–B6–B5	117.6(4)	C2R1–C2R5–C2R4	108.1(5)

Ni–Co iodo tetradecker product was seen. The best yields of **6**, up to 50% based on cobaltacarborane consumed, were obtained when a 2:1 ratio of $Cp^*Co(Et_2C_2B_3H_4I)$ to $NiBr_2$ was employed; in most experiments, substantial amounts (ca. 25–35%) of the carborane reagent were recovered. There is evidence that the $NiBr_2$ functions at least in part catalytically: 0.05 equiv gave **6** in 21% yield (34% based on cobaltacarborane consumed) over a 72-h period. When the reagent ratio was 1:1, no dimer or other products were observed. Reactions employing other nickel(II) halides ($NiCl_2$, NiF_2, NiI_2) produced **6** in low yields (<5%), and again no tetradecker complexes were found.

In contrast to the $NiBr_2$ reaction, treatment of **1e** with cobalt(II) halides generated B,B′-dihalo Co–Co–Co tetradecker sandwiches **7** (Scheme III). As shown, the iodo substituent was replaced by Cl or Br when $CoCl_2$ or $CoBr_2$ were employed, affording the known dichloro and dibromo species[2a] **7a** and **7b** and the previously unreported diiodo compound **7c**, all of which are paramagnetic and do not exhibit useful NMR spectra (**7a** has been characterized via X-ray crystallography[2a]). Since the chloro and bromo double-decker complexes **1a** and **1b** were not obtained in this reaction, **7a** and **7b** evidently formed via halogen exchange on the iodo tetradecker **7c**; this is further supported by a separate observation that treatment of **7c** with $CoCl_2$ and *tert*-butyllithium gave **7a**. Curiously, no evidence of dimer formation was seen in the synthesis of tetradeckers depicted in Scheme III.

The dimer **6**, which has no iodo substituents, was characterized by NMR, IR, UV–visible, and mass spectroscopy, but an X-ray diffraction study was required to establish its precise geometry. The crystal structure data and molecular parameters are listed

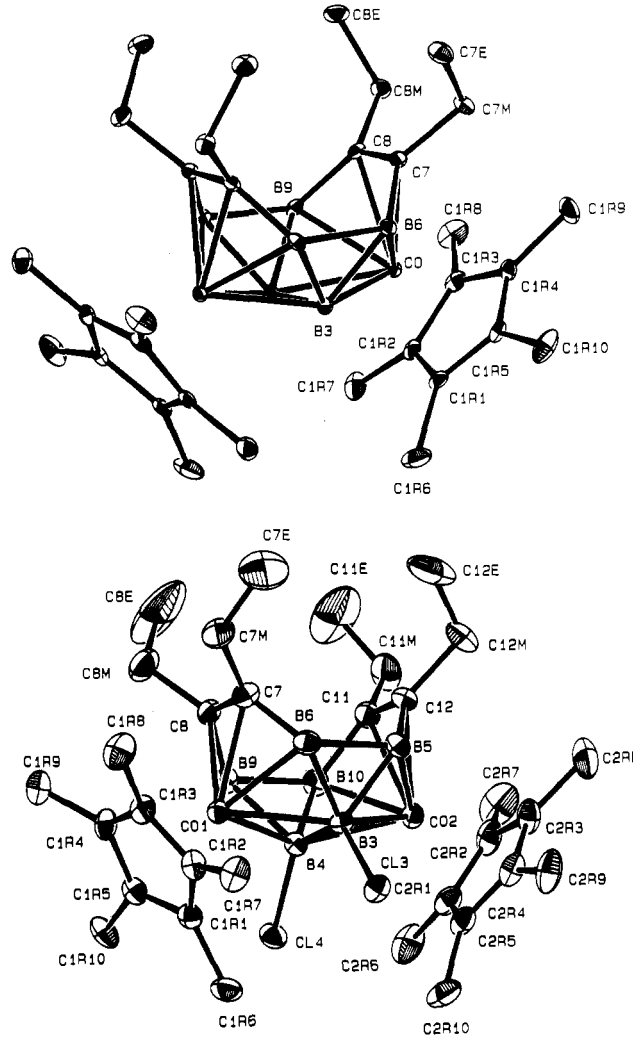

Figure 1. Molecular structures of $Cp^*_2Co_2Et_4C_4B_6H_6$ (**3a**) (top) and $Cp^*_2Co_2Et_4C_4B_6H_4Cl_2$ (**3d**) (bottom). Hydrogen atoms are omitted for clarity.

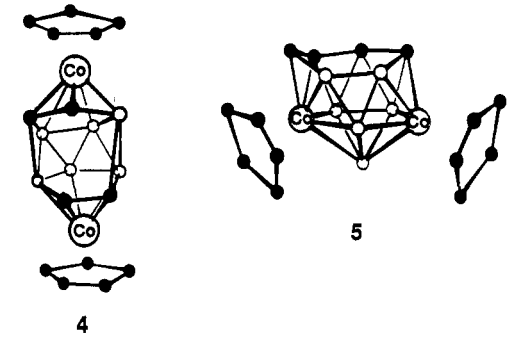

Figure 2. Structures of $Cp_2Co_2Me_4C_4B_6H_6$ (**4**)[4b] and $Cp_2Co_2C_4B_6H_{10}$ (**5**).[4a]

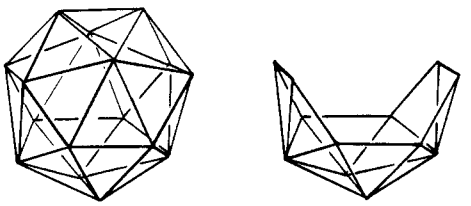

Figure 3. 16-vertex T_d polyhedron and fragment formed by removal of top 4 vertices.

Scheme III

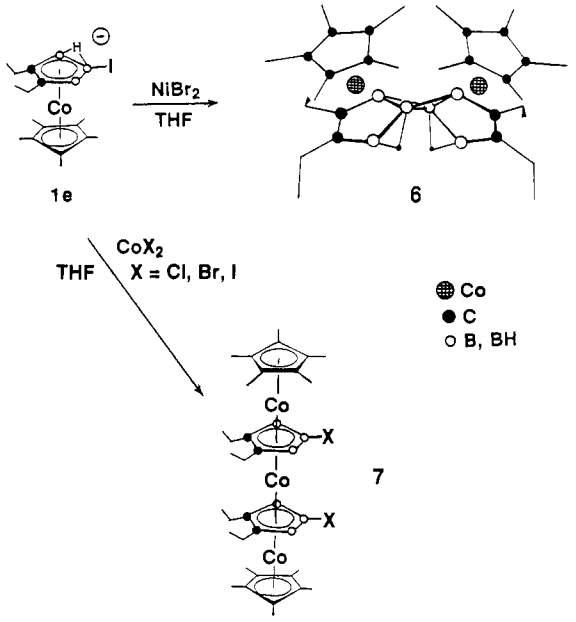

Table V. Bond Distances and Selected Bond Angles for $[Cp^*Co(Et_2C_2B_3H_3)]_2$, Bent Isomer (**6**)

	Bond Distances, Å		
Co1–C2	2.064(5)	C3–B4	1.519(7)
Co1–C3	2.093(4)	C1R1–C1R2	1.402(8)
Co1–C1R1	2.068(5)	C1R1–C1R5	1.413(7)
Co1–C1R2	2.027(5)	C1R1–C1R6	1.501(9)
Co1–C1R3	2.077(5)	C1R2–C1R3	1.401(8)
Co1–C1R4	2.078(5)	C1R2–C1R7	1.533(8)
Co1–C1R5	2.073(5)	C1R3–C1R4	1.414(8)
Co1–B4	2.117(5)	C1R3–C1R8	1.470(8)
Co1–B5	2.006(5)	C1R4–C1R5	1.420(7)
Co1–B6	2.055(6)	C1R4–C1R9	1.490(8)
C2M–C2	1.525(7)	C1R5–C1R10	1.493(7)
C2M–C2E	1.472(8)	B4–B5	1.760(7)
C2–C3	1.425(7)	B4–B5*	1.832(7)
C2–B6	1.528(9)	B5–B5*	1.65(1)
C3M–C3	1.526(6)	B5–B6	1.819(7)
C3M–C3E	1.333(8)		
	Selected Bond Angles, deg		
C2–C2M–C2E	111.9(5)	B4*–B5–B4	115.3(4)
C2M–C2–C3	123.4(5)	B4–B5–B6	100.5(4)
C2M–C2–B6	121.7(5)	B4*–B5–B6	142.6(4)
C3–C2–B6	114.7(4)	B5*–B5–B6	134.2(3)
C3–C3M–C3E	117.7(6)	C2–B6–B5	103.5(4)
C2–C3–C3M	121.1(4)	C1R2–C1R1–C1R5	107.7(5)
C2–C3–B4	116.9(4)	C1R1–C1R2–C1R3	109.2(4)
C3M–C3–B4	121.6(5)	C1R2–C1R3–C1R4	107.3(4)
C3–B4–B5	104.3(4)	C1R3–C1R4–C1R5	108.1(4)
C3–B4–B5*	135.8(4)	C1R1–C1R5–C1R4	107.6(4)

in Tables II and V, respectively. As shown in Figure 4, the molecule consists of two $Cp^*Co(Et_2C_2B_3H_3)$ sandwich units, crystallographically related by a C_2 axis, that are joined via a 4-boron, two electron-pair interaction involving B4, B5, B4*, and B5*, which adopt a boat-type configuration. The dihedral angle

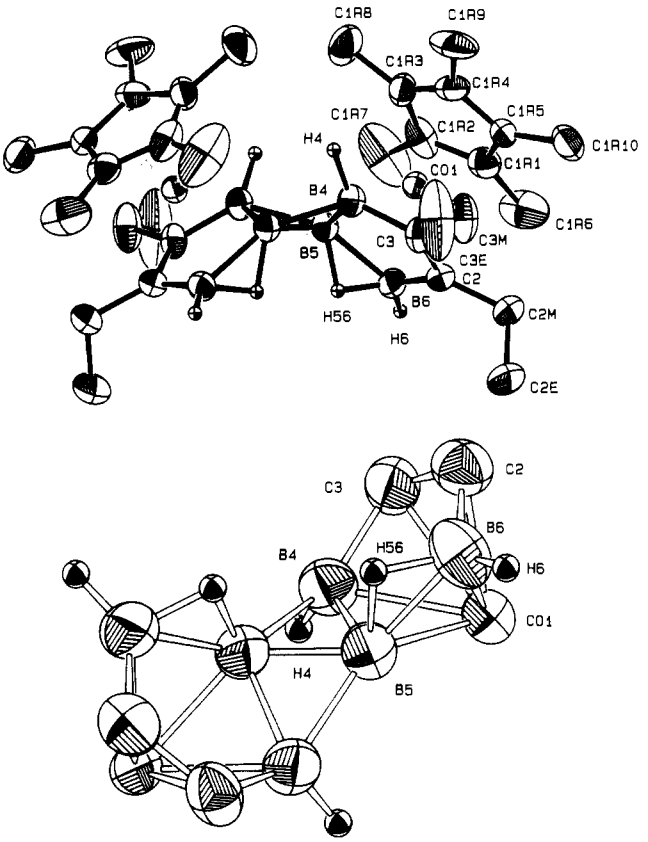

Figure 4. Top: Molecular structure of $[Cp^*Co(Et_2C_2B_3H_3)]_2$, bent isomer (**6**), with alkyl hydrogens omitted by clarity. Bottom: Detailed view of $Co_2C_4B_6$ framework.

between the C2–C3–B4–B5–B6 carborane ring and its rotational counterpart is 100°. The two groups exhibit normal bond distances and angles for *nido*-CoC_2B_3 clusters.[11] Each unit retains one bridging and two terminal hydrogens, and the linkage between them can be described in terms of a pair of three-center B–B–B bonds, discussed below.

The "twisted" conformation of the two cobaltacarborane units in **6** is ascribed to steric crowding of the Cp* ligands, which forces the CoC_2B_3 units to bend away from each other. This implies that if the two $Cp^*CoC_2B_3$ moieties were connected in a trans rather than cis configuration, coplanarity of the carborane rings would be possible. Fortuitously, we have isolated and structurally characterized the trans isomer (**8**) as a minor product of the reaction of the anion $\mathbf{1}^-$ with cobalt(II) chloride and cobaltocene, which as reported earlier[2a] afforded the parent tetradecker sandwich $[Cp^*Co(Et_2C_2B_3H_3)]_2Co$ (**11**) by crystallization from hexane solution without contact with silica. When a different portion of the original reaction mixture was chromatographed on silica in air, the complexes $[Cp^*Co(Et_2C_2B_3H_3]_2$ (**8**), $[Cp^*Co(Et_2C_2B_3H_4]_2$ (**9**), and $Cp^*Co(Et_2C_2B_3H_3)CoCp$ (**10**) were isolated in yields of 10, 25, and 25% respectively (Scheme IV). The proposed structures of **8–10** are supported by NMR and mass spectra. In the case of **9**, the presence of four bridging and four terminal hydrogen atoms probably precludes modes of intercage linkage other than a single B–B bond, as shown.

The dimer **8**, with two fewer hydrogens than **9**, is isomeric with **6**, and X-ray diffraction data (see Tables II and VI) show it to have an edge-fused geometry with a crystallographic center of symmetry, which constrains the two C_2B_3 rings to be coplanar

(11) (a) Benvenuto, M. A.; Sabat, M.; Grimes, R. N. *Inorg. Chem.* **1992**, *31*, 3904. (b) Piepgrass, K. W.; Stockman, K. E.; Sabat, M.; Grimes, R. N. *Organometallics* **1992**, *11*, 2404. (c) Pipal, J. R.; Maxwell, W. M.; Grimes, R. N. *Ibid.* **1978**, *17*, 1447. (d) Finster, D. C.; Grimes, R. N. *Ibid.* **1981**, *20*, 863. (e) Borodinsky, L.; Sinn, E.; Grimes, R. N. *Ibid.* **1982**, *21*, 1928.

Scheme IV

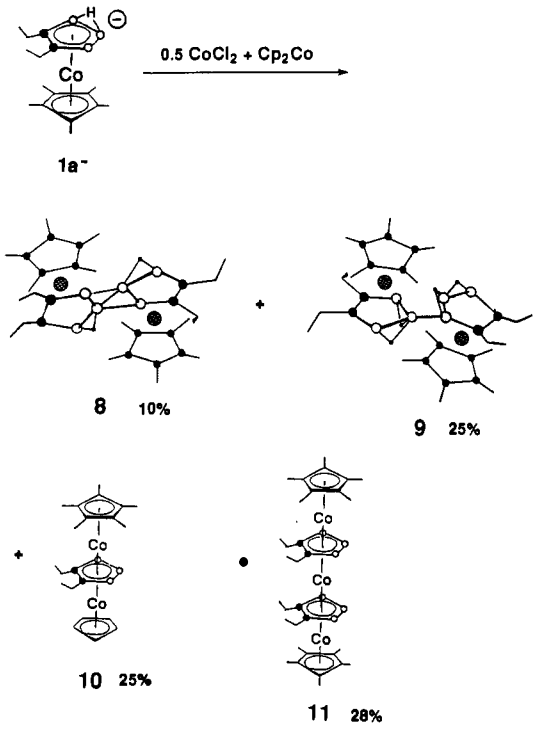

Table VI. Bond Distances and Selected Bond Angles for $[Cp^*Co(Et_2C_2B_3H_3)]_2$, "Planar" Isomer (**8**)

	Bond Distances, Å		
Co–C2	2.064(3)	C1R1–C1R5	1.427(4)
Co–C3	2.064(3)	C1R1–C1R6	1.490(4)
Co–C1R1	2.061(3)	C1R2–C1R3	1.421(4)
Co–C1R2	2.049(3)	C1R2–C1R7	1.503(4)
Co–C1R3	2.067(3)	C1R3–C1R4	1.430(4)
Co–C1R4	2.075(3)	C1R3–C1R8	1.495(4)
Co–C1R5	2.081(3)	C1R4–C1R5	1.428(4)
Co–B4	2.062(4)	C1R4–C1R9	1.499(4)
Co–B5	2.085(3)	C1R5–C1R10	1.492(4)
Co–B6	2.042(3)	B4–B5	1.812(5)
C2–C2M	1.518(4)	B4–H4	1.07(3)
C2–C3	1.435(4)	B4–H45	1.26(3)
C2–B6	1.533(4)	B5–B6	1.774(5)
C2M–C2E	1.525(4)	B5–B6*	1.843(4)
C3M–C3	1.514(4)	B5–H5	1.12(3)
C3M–C3E	1.533(4)	B5–H45	1.22(3)
C3–B4	1.517(5)	B6–B6*	1.639(6)
C1R1–C1R2	1.436(4)		
	Selected Bond Angles, deg		
C2–C2M–C2E	112.1(3)	B6–B5–H5	145(1)
C2M–C2–C3	122.1(2)	H5–B5–H45	108(2)
C2M–C2–B6	122.7(3)	B6–B5–H45	103(1)
C3–C2–B6	114.4(3)	B6*–B5–H5	99(1)
C3–C3M–C3E	110.3(3)	B6*–B5–H45	112(1)
C2–C3–C3M	122.8(3)	C2–B6–B5	107.8(2)
C2–C3–B4	113.4(2)	C2–B6–B5*	120.0(3)
C3M–C3–B4	123.5(3)	C2–B6–B6*	153.3(4)
C3–B4–B5	107.9(2)	B5–B6–B5*	126.2(2)
C3–B4–H4	127(2)	C1R2–C1R1–C1R5	107.7(3)
C3–B4–H45	112(1)	C1R1–C1R2–C1R3	108.3(2)
B5–B4–H4	124(2)	C1R2–C1R3–C1R4	107.7(3)
H4–B4–H45	114(2)	C1R3–C1R4–C1R5	108.3(2)
B4–B5–B6	96.4(2)	C1R1–C1R5–C1R4	107.9(2)
B4–B5–H5	117(1)		

(Figure 5). As in the case of its isomer **6**, the individual CoC_2B_3 cluster units exhibit normal geometric parameters. The intercage distances B5–B6* and B5*–B6 are 1.843(4) Å, well within the range of B–B covalent bonding and only slightly longer than the intracage B5–B6 distance of 1.774(5) Å; the length of the "diagonal" bond B6–B6* is 1.639(6) Å. The two rings are therefore effectively fused into a planar 10-atom C_4B_6 bicyclic

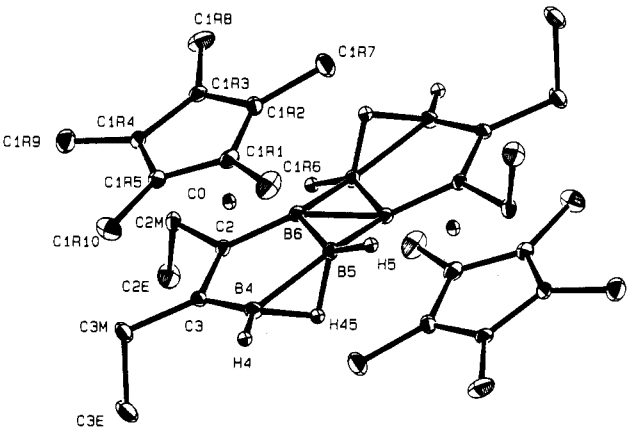

Figure 5. Molecular structure of "planar" isomer of $[Cp^*Co(Et_2C_2B_3H_3)]_2$ (**8**) with alkyl hydrogens omitted for clarity.

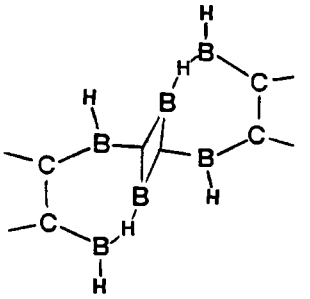

Figure 6. Valence-bond description of the formal $Et_4C_4B_6H_6^{4-}$ unit in **8**, showing linkage via two 3-center bonds. Electrons and atomic orbitals involved in bonding to the two Cp^*Co^{2+} moieties (12 and 10, respectively) are not shown.

system, formally represented as $Et_4C_4B_6H_6^{4-}$, to which a pair of $Cp^*Co(III)^{2+}$ units are η^5-coordinated on opposite sides of the ring plane. As far as we are aware, this is the first known example of planar fusion of two carborane rings.

The $Cp^*Co(Et_2C_2B_3H_3)$ moieties in **6** and **8** each contain two fewer electrons than their neutral precursors (by virtue of the formal loss of 2 H·) and are therefore coordinately unsaturated, a situation that is remedied by dimerization via two intercage B–B bonds. A valence-bond description involving a pair of 3-center interactions, consistent with the numbers of available electron pairs and orbitals, is shown in Figure 6.

General Observations

In contrast to our studies on the rational synthesis of organotransition-metal metallacarboranes,[3b,11b,12] the fusion chemistry described in this paper is comparatively unpredictable and the operative mechanisms can only be speculated upon at this point. It is clear that transition metal-mediated reactions of small metallacarborane substrate anions can generate a variety of linked, edge-fused, and fully fused products in which the mediating metal is absent, as well as multidecker sandwiches in which the metal is incorporated. There is no doubt that the processes by which these various species are generated are closely related and can even occur in the same reaction system, as the reaction in Scheme IV clearly demonstrates. The course of reaction is influenced not only by the choice of metal reagent, substituents on the metallacarborane precursor, and reaction conditions but by the method of workup as well.

Linkage of metallacarborane clusters through single B–B, B–C, or C–C bonds is proving more straightforward, and we are in the

(12) (a) Davis, J. H., Jr.; Sinn, E.; Grimes, R. N. *J. Am. Chem. Soc.* **1989**, *111*, 4776. (b) Davis, J. H., Jr.; Sinn, E.; Grimes, R. N. *Ibid.* **1989**, *111*, 4784. (c) Piepgrass, K. W.; Grimes, R. N. *Organometallics* **1992**, *11*, 2397. (d) Davis, J. H., Jr.; Attwood, M. D.; Grimes, R. N. *Organometallics* **1990**, *9*, 1171.

process of developing controlled synthetic routes to such species. Several preliminary reports have appeared,[13] and forthcoming papers will describe the application of Wurtz-type and similar reactions to this chemistry.[14]

Experimental Section

Except where otherwise stated, materials, instrumentation, and procedures were as given in earlier publications.[2] Mass spectra of all new compounds gave strong parent envelopes that were in good agreement with calculated intensities based on natural isotopic distributions. Elemental analyses were obtained either in this department on a Perkin-Elmer 2400 CHN analyzer using cyclohexanone-2,4-dinitrophenylhydrazone as a standard (we thank Kenneth Stockman for performing the analyses) or by E&R Microanalytical Laboratory, Corona, NY 11368. Column chromatography was conducted on silica gel 60 (Merck), and thick-layer chromatography was carried out on precoated silica gel plates (Merck). Dichloromethane and *n*-hexane were anhydrous grade and were stored over 4-Å molecular sieves prior to use. THF was distilled from sodium–benzophenone immediately prior to use. The *nido*-$Cp^*Co(Et_2C_2B_3H_4$-5-X) complexes **1a–d** were prepared as described elsewhere.[11b,12c,d] Unless otherwise indicated, all syntheses were conducted under vacuum or an atmosphere of nitrogen. Workup of products was conducted in air using benchtop procedures.

Synthesis of $Cp^*_2Co_2Et_4C_4B_6R_6$ (3a–c). For **3a** (R = H), a 314-mg (1.00-mmol) sample of $Cp^*Co(Et_2C_2B_3H_5)$ (**1a**) was placed in a 3-neck 100-mL flask which was fitted with a septum and attached to a vacuum line. Iron(II) chloride (64 mg, 0.50 mmol) was placed in a tip tube and attached to the third neck. About 30 mL of dry THF was condensed into the reactor in a liquid-nitrogen bath under vacuum, and the flask was placed in a dry ice/ethanol bath. To this solution was added, via syringe, 0.4 mL of 2.5 M *tert*-butyllithium in hexane. The solution was warmed to room temperature and stirred for 30 min, during which the color changed from yellow to deep red–orange. The $FeCl_2$ was tipped in, causing a rapid color change to dark brown (within seconds) and to black in 30 min. The solution was stirred for 3 h at room temperature, after which it was opened to the air and the solvent was removed. The residue was taken up in hexane and washed through 2 cm of silica, first with hexane and then with CH_2Cl_2. The hexane wash was column-chromatographed to give starting material (186 mg, 59% recovery). The CH_2Cl_2 fraction was column-chromatographed on silica TLC plates in 1:1 hexane:CH_2Cl_2, yielding five bands of which all except the second were minor. The second band was black and was extracted with CH_2Cl_2 and solvent removed, affording 20 mg of black solid **3a** (0.032 mmol, 16% based on **1a** consumed). Visible–UV absorptions (nm, in CH_2Cl_2): 444 (11%), 350 (53%), 308 (88%), 264 (100%). Anal. Calcd for $Co_2C_{32}B_6H_{56}$ (**3a**): C, 61.64; H, 9.05. Found; C, 60.79; H, 9.67.

For **3b** (R = Me), the same procedure was followed by employing the 5-methyl derivative **1b** (311 mg, 0.95 mmol), 0.38 mL of 2.5 M butyllithium, and 60 mg (0.48 mmol) of $FeCl_2$. The hexane fraction from the silica washing was chromatographed on silica TLC plates in pentane, giving one major yellow band, which was **1b** (170 mg, 57% recovery), identified from its mass spectrum (cutoff at m/z 651). For **3c** (R = Et), the same procedure was employed using the 5-ethyl derivative **1c** (355 mg, 1.04 mmol), 0.42 mL of 2.5 M butyllithium, and 64 mg (0.50 mmol) of $FeCl_2$. Workup as before gave **1c** from the hexane fraction (170 mg, 57% recovery). The CH_2Cl_2 fraction from the silica washing was chromatographed on silica in 10:1 hexane:CH_2Cl_2, affording four bands of which the last to elute was a few milligrams of purple **3c** (m/z 679).

Synthesis of $Cp^*_2Co_2Et_4C_4B_6H_4Cl_2$ (3d). In a procedure analogous to that previously employed[2a] in the synthesis of the tetradecker complex $[Cp^*Co(2,3\text{-}Et_2C_2B_3H_2\text{-}5\text{-}Cl)]_2Ni$, the apparatus used in the preparation of **3a** was charged with 200 mg (0.57 mmol) of the 5-chloro complex $Cp^*Co(Et_2C_2B_3H_4Cl)$ (**1d**) and 37 mg (0.29 mmol) of iron(II) chloride. About 60 mL of dry THF was condensed into the reactor immersed in a liquid-nitrogen bath under vacuum, and the flask was warmed to ice water temperature. To this solution was added, via syringe, an equimolar amount of *tert*-butyllithium in hexane. The solution immediately turned orange with formation of the anion and was warmed to room temperature with no further color change. After 30 min, the solution was cooled to 0 °C and the $FeCl_2$ was tipped in; the color changed rapidly (2 min) to dark brown. The solution was warmed to room temperature and stirred for 4 h, after which it was opened to the air and the solvent was removed. The residue was taken up in hexane and washed through 2 cm of silica, first with hexane and then with CH_2Cl_2. The hexane wash was column-chromatographed to give starting material (122 mg, 61% recovery). The CH_2Cl_2 wash was column-chromatographed in 1:1 hexane:CH_2Cl_2, yielding two bands, of which the first was dark brown **3d** (34 mg, 0.049 mmol, 44% based on **1d** consumed). The second band was black and consisted of unidentified products; a mass spectrum of this material gave a parent peak at m/z 750 (calculated high mass peak for a Co–Fe–Co dichloro tetradecker complex would appear at 748 amu). Visible–UV absorptions for **3d** (nm, in CH_2Cl_2): 476 (16%), 374 (58%), 320 (73%), 300 (82%), 282 (100%), 256 (83%). IR (neat film, cm^{-1}): 2960 s, 2924 vs, 2854 s, 2421 m, 2361 m, 1734 m, 1457 m, 1375 m, 1071 w, 1011 m, 951 w, 805 m, 697 m. Anal. Calcd for $Co_2Cl_2C_{32}B_6H_{54}$: C, 55.51; H, 7.86. Found: C, 55.16; H, 8.16.

Synthesis of $[Cp^*Co(Et_2C_2B_3H_3)]_2$, Bent Isomer (6). In a typical procedure, $Cp^*Co(Et_2C_2B_3H_4I)$ (220 mg, 0.50 mmol) and $NiBr_2$ (55 mg, 0.25 mmol) were placed in a 100-mL round-bottom flask equipped with a septum and evacuated on a vacuum line. The flask was cooled in liquid nitrogen, and ca. 50 mL of dry THF was condensed in. The flask was warmed to 0 °C, and 0.10 mL of 1.7 M *tert*-butyllithium (0.17 mmol) was added through the septum. The 0 °C bath was removed and the solution stirred for 45 min, after which the flask was again cooled to 0 °C and another 0.10-mL portion of butyllithium was added. The cycle was repeated until a total of 0.40 mL (0.68 mmol) of *tert*-butyllithium was injected. The flask was stirred for 1 h and opened to air, and the solvent was removed by rotary-evaporation. The residue was taken up in CH_2Cl_2 and washed through 2 cm of silica, and the filtrate was taken to dryness. The residue was column-chromatographed on silica with hexane as eluent. Three bands were obtained, the first of which was a trace of $Cp^*Co(Et_2C_2B_3H_5)$, while the second was starting material (61 mg, 28% recovery). The third band was orange **6** (31 mg, 0.050 mmol, 28% based on starting complex consumed). In other experiments, isolated yields up to 50% were obtained. Visible–UV absorptions for **6** (nm, in CH_2Cl_2): 486 (7%), 390 (26%), 320 (99%), 294 (100%), 274 (95%), 242 (78%). IR (neat film, cm^{-1}): 2960 vs, 2920 vs, 2863 s, 2500 vs, 2000 br w, 1445 m, 1428 s, 1377 vs, 1303 w, 1027 s, 929 m, 784 w, 734 w. Anal. Calcd for $Co_2C_{32}B_6H_{56}$: C, 61.64; H, 9.05. Found: C, 61.23; H, 9.24.

Synthesis of $[Cp^*Co(Et_2C_2B_3H_2\text{-}5\text{-}X)]_2Co$ Tetradecker Complexes (7a, X = Cl; 7b, X = Br; 7c, X = I) from $Cp^*Co(Et_2C_2B_3H_3I)^-$. In a procedure analogous to that previously described for the synthesis of B(5),B(5′)-dihalo tetradecker complexes[2a] (and essentially the same as the preparation of **3d** given above), 200 mg (0.45 mmol) of $Cp^*Co(Et_2C_2B_3H_4$-5-I) (**1e**) was reacted in THF with 0.5 equiv of $CoCl_2$, $CoBr_2$, or CoI_2. Workup as before, with separation of products into CH_2Cl_2 and hexane fractions followed by chromatography on silica, gave respectively the known species[2a] **7a** and **7b** and the diiodo tetradecker **7c**, identified by proton NMR and mass spectroscopy; in each case, a large portion of the starting material **1e** was recovered. Isolated yields: from $CoCl_2$, 36% **1e** and 32% **7a**; from $CoBr_2$, 54% **1e** and 20% **7b**; from CoI_2, 46% **1e** and 24% **7c**. The proton NMR and mass spectra of the tetradecker products indicated, in each case, the presence of both metal-protonated and unprotonated forms (i.e., the central metal unit can be Co or CoH), which were not separable on chromatography.

Synthesis of $[Cp^*Co(Et_2C_2B_3H_3)]_2$, "Planar" Isomer (8), and $[Cp^*Co(Et_2C_2B_3H_4)]_2$ (9). These compounds were isolated as yellow solid byproducts of the synthesis of the parent tetradecker complex **11** via the reaction of $Cp^*_2Co(Et_2C_2B_3H_4)^-$ ion (**1d**$^-$) with $CoCl_2$ and cobaltocene, the details of which have been presented elsewhere.[2a] The brown-red triple-decker $Cp^*Co(Et_2C_2B_3H_3)CoCp$ (**10**) was also obtained in ca. 25% yield and characterized from its NMR and mass spectra. Data for **8**: yield 138 mg (0.22 mmol, 11% based on **1a** consumed). Anal. Calcd for $Co_2C_{32}B_6H_{56}$: C, 61.64; H, 9.05. Found: C, 61.80; H, 9.31. Data for **9**: yield 329 mg (0.53 mmol, 25% based on **1a** consumed). Anal. Calcd for $Co_2C_{32}B_6H_{58}$: C, 61.44; H, 9.35. Found: C, 61.24; H, 9.53.

X-ray Structure Determinations. Measurements on **3a** and **8** were carried out on a Rigaku AFC6S diffractometer at −120 °C, while those on **3d** and **6** were obtained on a Siemens/Nicolet P3m unit at 25 °C. Mo Kα radiation was employed in all cases. Table II lists information on the data collection and structure determinations. Unit cell dimensions were obtained using the setting angles of 25 high-angle reflections. The intensities of three standard reflections were monitored, showing neither

(13) (a) Piepgrass, K. W.; Wang, X.; Meng, X.; Sabat, M.; Grimes, R. N. *Abstracts of Papers*, 204th National Meeting of the American Chemical Society, Washington, DC; American Chemical Society: Washington, DC, 1992; Abstract INOR 431. (b) Wang, X.; Piepgrass, K. W.; Curtis, M. A.; Sabat, M.; Grimes, R. N., *Abstracts* of *Papers*, Third Boron-USA Workshop, Pullman, WA, July 1992; Abstract No. 52.

(14) Wang, X.; Meng, X.; Sabat, M.; Grimes, R. N. Manuscript in preparation.

significant decay nor instrument instability. For compounds **3a**, **3d**, and **8**, empirical absorption corrections were applied based on the ψ scans of several reflections. In the case of **6**, absorption corrections were applied via the program DIFABS.[15] All calculations were performed on a VAXstation 3520 computer using the program TEXSAN 5.0.[16] The structures of **3a**, **6**, and **8** were solved by direct methods (SIR88[17]), and that of **3d**, by heavy-atom techniques. Full-matrix least-squares calculations with anisotropic thermal displacement parameters for all nonhydrogen atoms were carried out for each structure. Hydrogen atoms were located from difference Fourier maps and included as fixed contributions to the structure factors. The final difference Fourier maps were featureless, with the highest peaks listed in Table II. Scattering factors were those of Cromer and Waber[18] with anomalous dispersion corrections from Ibers and Hamilton.[19]

Acknowledgment. This work was supported by the U.S. Army Research Office and the National Science Foundation, Grant No. CHE 9022713.

Supplementary Material Available: Tables of positional and anisotropic thermal parameters and mean planes (15 pages). Ordering information is given on any current masthead page.

(15) Walker, N.; Stuart, D. *Acta Crystallogr.* **1983**, *A39*, 158.
(16) TEXSAN 5.0: Single Crystal Structure Analysis Software. Molecular Structure Corp., The Woodlands, TX 77381, 1989.
(17) SIR88: Burla, M. C.; Camalli, M.; Cascarano, G.; Giacovazzo, C.; Polidori, G.; Spagna, R.; Viterbo, D. *J. Appl. Crystallogr.* **1989**, *22*, 389.
(18) Cromer, D. T.; Waber, J. T. In *International Tables for X-Ray Crystallography*; Kynoch Press: Birmingham, U.K., 1974; Vol. 1, pp 71–78.
(19) Ibers, J. A.; Hamilton, W. C. *Acta Crystallogr.* **1964**, *A17*, 781.